2002070

Finite Element Impact Modelling for Shot Peen Forming

Tao Wang, Jim Platts
University of Cambridge, Cambridge, UK
Andrew Levers
Airbus UK Ltd, Chester, UK

1 Abstract

A finite element analysis of multiple random impacts involved in shot peen forming is presented. An explicit dynamic algorithm for modelling up to 1000 impacts and a static algorithm for spring-back simulation are combined to achieve a final curved shape after shot peening on a small sized aluminium 2024-T351 sample. The development of the plastic zones, residual stresses, and the final deflection is given by simulating the experimental conditions. The comparison between simulation results and experiments shows that the finite element impact modelling is able to investigate the macroscopic effects (e.g. curvature) of shot peening as well as the microscopic effects (e.g. local plasticity and residual stresses).

2 Introduction

Shot peening forming involves numerous randomly distributed impacts on the surface of metal sheet. The individual plastic zones created by each impact have a tendency to expand sideways and combine to curve the peened metal sheet and to induce residual stresses in it. For the understanding of peening mechanics, previous numerical work has progressed from the finite element simulation of single indentation or impact to multiple in-line or regularly distributed impacts.

Follansbee and Sinclair [1], and Sinclair et al [2] investigated the quasi-static indentation of an elastic-plastic half-space by a rigid sphere using an axis-symmetric finite element method. Meguid and Klair [3] modelled a plate co-indented by two smooth, flat, and rigid punches under plane-strain condition to investigate the interaction between two plastic zones. Grasty [4] modelled nine uniformly distributed indentations by 3D finite elements and extrapolated the deflection to be compared with experiments. Al-Obaid [5] developed a three-dimensional dynamic FE program to determine the residual stress and plasticity of the peened material by applying a dynamic patch load distributed on the target surface. Levers and Prior [6] suggested that the extrapolation of single shot impact to a realistic peening process is difficult and the dynamic explicit FEM for multiple impact modelling is attractive in its efficiency and application to practical peening processes. Nevertheless, they found that the explicit method is truly dynamic so that the model can not reach a state of static equilibrium by simply extending the computation time. Therefore, they finally introduced a temperature profile approach based on shell elements to model the residual stress profile through thickness and hence the corresponding macroscopic deflection.

None of these investigations, however, has dealt with the problem of randomly distributed impacts, which are physically involved in shot peening processes. It is also worth noting that the

investigation of peen forming processes has concentrated on the macroscopic effect of shot peening by neglecting individual impacts based on shell assumption [6~10]. However, if peening mechanics is concerned, a 3D FEA is preferred because the normal impact pressure is actually the most important load to induce the resulting effects.

Particular attention was therefore devoted to two steps: (1) Verify the feasibility of combining dynamic and static FE algorithms together for modelling numerous randomly distributed impacts in peen forming to calculate the final curved shape. (2) Obtain the overall trend of the development of peen formed curvatures, plasticity, and residual stresses.

3 The Experiment

Aluminium 2024-T351 sheets are used for this study. Square samples 20 × 20 mm with 4mm nominal thickness are chosen because the distribution of peens within this surface area can be approximated as a uniform distribution for the peening machine being used. However, for larger surface areas a Gaussian distribution was expected by Holdgate [11].

Cast steel S660 peens are used in an air-blast machine. The mass flow rate is kept as a constant 13.67 g/s and the air pressure is adjustable from 20 psi to 50 psi and exposure time from 10 s to 25 s. The nozzle is kept vertical to the worktable at a distance of 300 mm. Unlike Almen tests, specimens are not constrained by a holder during peening. Instead, only adhesive materials (e.g. tapes) around the test pieces are used to prevent the specimen from moving laterally due to air blast. Therefore, the specimen is unconstrained and is free to bend and elongate.

After peening, the specimen is cold mounted in an acrylic material to preserve the deformed configuration. It is then cut through thickness near the initial diagonal of the square surface in a precision cutting machine. The section is finally ground down to a grit size of 1200 for the measurement of deflection and micro-hardness in a micro-indentation machine. The curvature is determined by approximating the measured points with a second order polynomial function. A convenient method to measure the curvature is to measure a number of points on the unpeened bottom surface by a coordinate measurement machine and to approximate these points by a sphere. These two methods give similar results. When measuring the deflection by both methods, measurement points are taken at an approximate distance equal to the sample thickness away from the edge.

4 The Finite Element Analysis

The finite element package ABAQUS is used to simulate the procedure corresponding to the experimental operation. Because of its efficiency, the Explicit dynamic algorithm is used to simulate the numerous impacts. However, as stated above, since a static solution is necessary, the Standard static algorithm is combined to provide the resulting deformed shape as a spring-back analysis.

Steel S660 shots are assumed as spherical rigid surfaces since they are harder than the aluminium target sheet. In addition, the analytical rigid surface gives a good computational efficiency. Each shot is associated with a mass element and a rotary inertial element, which are calculated according to the density of the shot and its spherical volume. The shot density ρ is given by 7500 kg/m^3 and the shot radius R is 0.968 mm as the average of those measured by a number of

randomly selected shots. The simulated velocity v is from 21~35 m/s estimated for the experimental machine [11] under the given air pressure and mass flow rate. The velocity is assumed to be in the vertical direction and applied to each shot as an initial condition. No other translation and rotation velocities are applied to shot.

The aluminium 2024-T351 target sheet is modelled by only a quarter to save computation cost. The elements used are 3D continuum elements C3D4. At least 9 elements are arranged through the thickness. The element dimensions in the target plane are uniform 0.3 × 0.3 mm. 0.2 × 0.2 mm dimensions are also used for detailed coverage investigation. The material property of the sheet is defined by its uni-axial tensile test, regardless of the rolling direction and the dependence on strain-rate. Its stress-strain relationship is approximated by a power function. Corresponding to the unconstrained peening in experiments, a rigid surface is arranged under the target sheet to provide support. The friction coefficient between them is assumed as 0.4. A program is written to create 3D uniformly random distributed shots over the top surface of the sheet to model the shot stream. Up to 1000 shots can be simulated in the current study. The friction coefficient between each shot and the sheet is also assumed as 0.4.

5 Results and Discussion

5.1 The Development of Curvature

The impact velocity is determined by measuring the indentation diameter on 2 mm thick aluminium 5251-H22 sheets after peening to a low coverage. The analytical results in Wang[12] and experimental results for the same material in Holdgate [11] can be used to estimate the impact velocity. The estimated velocity is very similar to the one measured for a sister machine at Airbus UK [13]. In addition, in order to compare the macroscopic deflection from finite element model with experiments, the analysis time in FE analysis needs to be calibrated. Because the real time is too long for an explicit analysis, the FE analysis has to be accelerated by arranging one impact immediately after the other. Thus, the calibration of the FE analysis to experiments is needed. The calibration is conducted by comparing the curvature results from both FE analy-

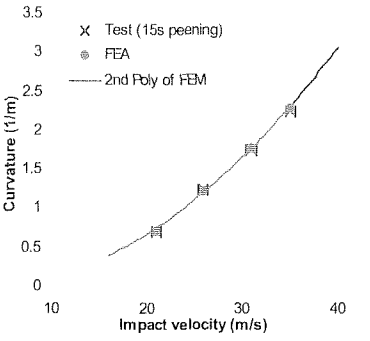

Figure 1: The comparison of FE analyses with experimental results for 15 s peening

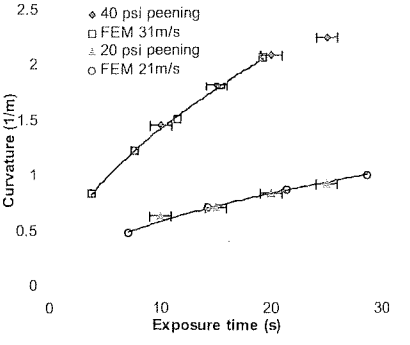

Figure 2: The comparison of FE analyses for 21 m/s and 31m/s impacts with experimental results for 20 psi and 40 psi peening

ses and experiments assuming the velocity determined by peening pressure is accurate. This gives a calibration factor of the FE analysis time to the real exposure time for the model being used, which is a function of the impact velocity. Based on the calibration, the comparison of FE analysis with experimental results is shown in Figure 1 for 15 s peening under different peening pressure and in Figure 2 for 20psi and 40psi peening under different exposure time.

5.2 The Development of Coverage

With the finite element model, the plastic coverage [14] can be calculated by analyzing the plastic region. However, to determine the plastic coverage is much more difficult than the visual coverage using experimental methods. The development of equivalent plastic strains on the impact surface for 31m/s impacts is given in Figure 3 from the finite element analysis. The minimum equivalent plastic strains are set to $7 \cdot 10^{-3}$, which is approximately 1 tenth of the representative strain $0.2 \cdot a/R$ [15] The black region indicates a high-plasticized zone and the white indicates an approximated non-plasticized zone. The surface plastic coverage was calculated by an image-processing program, which calculated the ratio of the plasticized area to the total area. The specific values are given under their corresponding diagrams. The development of the plastic coverage C_{pr} (FEA) together with the calculation of the visual coverage ratio [11, 16] is shown in Figure 4.

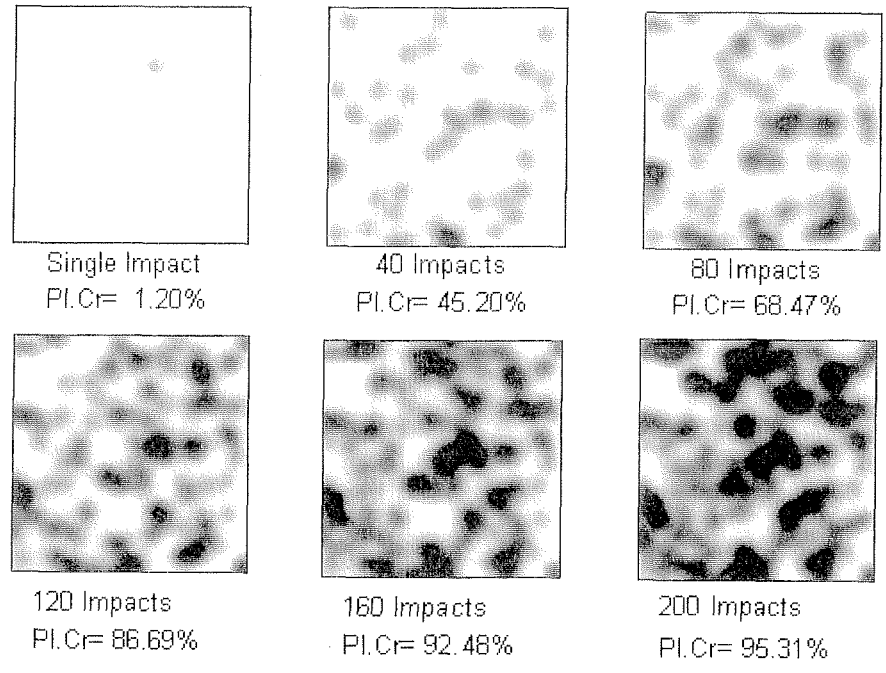

Figure 3: The development of the plastic coverage

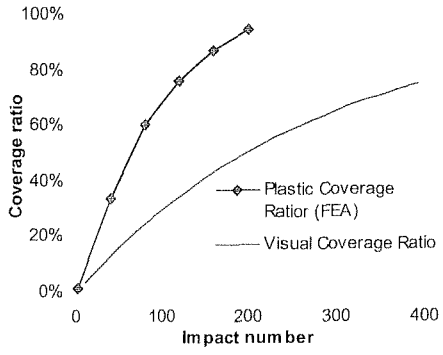

Figure 4: The comparison of the plastic coverage ratio with visual coverage ratio

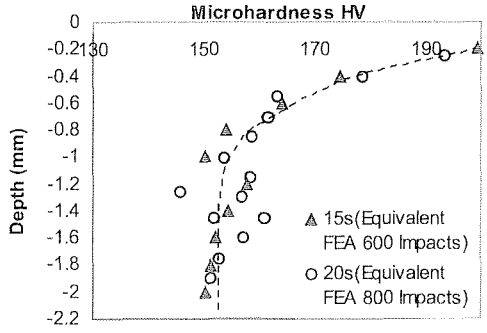

Figure 5: Experimental results of micro-indentation for 40 psi peening

The experimental microhardness values through the thickness of the peened sample are shown in Figure 5. The depth is measured from a local top of the peened surface under a 40× microscope. The FEA results of the through-thickness plasticity along the diagonal section is shown in Figure 6 for 100~800 impacts (31m/s) in the undeformed configuration for a clear view of the thickness. Both FEA and tests give an estimation of the plastic depth about 1~1.2 mm. It is worth noting that the analysis for a single impact [12] gives an estimation about 0.97 mm, which is not considerably changed by multiple impacts.

5.3 Residual Stresses

The development of the residual stress σ_x along the diagonal section is shown in Figure 7. The white colour indicates tensile stress field. The distribution of σ_y has a similar contour so it is not shown here. It is interesting to note that for a partial coverage (200 impacts, coverage ratio = 50~60 %) a large percent of the impacted surface is actually under a compression state. A compressed layer is clearly shown in this figure and it can be compared with the plastic layer shown in Figure 6.

6 Conclusions

The applicability of impact modelling to investigate the mechanics of shot peen forming on a small sized sample is demonstrated through the above analysis. The method of combining the dynamic explicit and static algorithm for a peen forming purpose is able to investigate the macroscopic effects of shot peening as well as microscopic effects. However, previous numerical work on impact modelling concentrated on microscopic effects, such as the residual stress and local plasticity. In fact, Kopp and Ball [17] argued that the quantitative calculation of residual stresses by axis symmetric single indentation or impact model is of little practical use and suggested further multiple impact modelling.

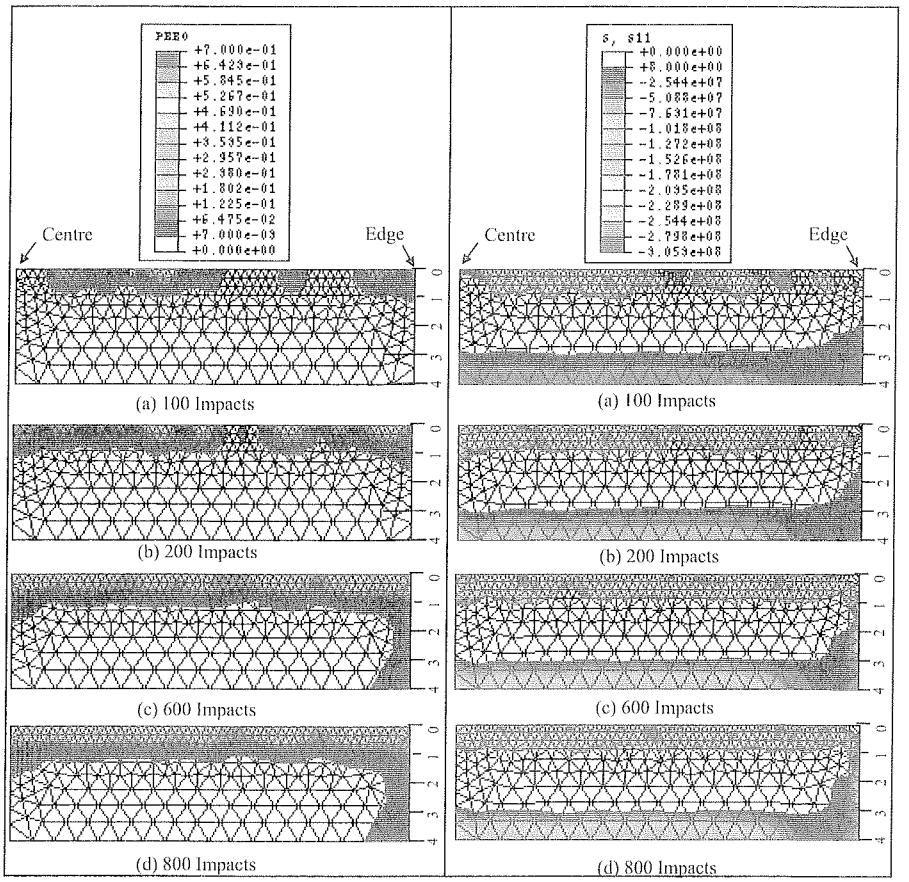

Figure 6: The development of the through-thickness plasticity

Figure 7: The development of residual stress σ_x

As Meguid [14] envisioned that the plastic coverage develops faster than the visual surface coverage, the finite element simulation gives a firm proof to his suggestion. In addition, a layer with compressive residual stresses develops as the plastic layer is formed. These discoveries can therefore be used to explain that partial-coverage peening to some extent could also enhance the fatigue strength of metals.

The layered structures, such as the plastic layer and the compressed layer, are clearly shown by the present FEA. Like Grasty's squeezed-layer model [4], a more efficient model by applying layered plastic deformation using shell elements for realistic sized components of peen forming is being considered.

7 References

[1] P. S. Follansbee & G. B. Sinclair, Int. J. Solids Structures, 1984, 20, 81–91

[2] G. B. Sinclair, P. S. Follansbee & K. L. Johnson, Int. J. Solids Structures, 1984, 21, 865–888.

[3] S. A. Meguid & M. S. Klair, J. Mech. Work. Tech., 1985, 11, 87–104.

[4] L. V. Grasty, PhD Thesis, Cambridge University, 1992.

[5] Y. F. Al-Obaid, Computers & Structures, 1994, 52, 693–703.

[6] A. Levers & A. Prior, J. Mat. Proc. Tech., 1998, 80, 304–308.

[7] R. D. VanLuchene & E. J. Cramer, J. Mat. Eng. Perf., 1996, 5, 753–760.

[8] X. M. Kang, T. He, Z. E. Ma & Y. M. Kong, J. Aero. Manufacturing Eng., 1997, 6.

[9] D. S. Gardiner & M. J. Platts, ICSP7, Institute of Precision Mechanics, Warsaw, 1999, 235–243.

[10] D. S. Gardiner, PhD Thesis, Cambridge University, 2001.

[11] N. M. D. Holdgate, PhD Thesis, Cambridge University, 1993.

[12] T. Wang, Internal Report, Cambridge University Engineering Department, 2001

[13] A. Levers, Personal communication, 2001

[14] S. A. Meguid, Fatigue & Fracture of Engineering Materials & Structures, 1991, 14, 515–530.

[15] D. Tabor, The Hardness of Metals, Clarendon Press, Oxford, 1951

[16] D. Lombardo & P. Bailey, ICSP6, San Francisco, USA, 1996, 493–503.

[17] R. Kopp & H. W. Ball, ICSP3, Deutsche Gesellschaft fur Metaukunde, Garmisch Partenkirchen, 1987, 298–307.